文章编号：0258-7106 (2020) 04-0631-16 Doi: 10. 16111/j. 0258-7106. 2020. 04. 008

江西永平 Cu-W 矿床白钨矿地球化学特征及其对矿床成因的指示*

苏蔷薇[1],毛景文[1],宋世伟[1],王训军[2]

（1 中国地质科学院矿产资源研究所 自然资源部成矿作用与资源评价重点实验室,北京 100037;
2 江西铜业股份有限公司,江西 上饶 334506）

摘 要 江西永平 Cu-W 矿床是钦杭成矿带东部一个大型 Cu-W 矿床。针对该矿床的成因,一直存在着海底喷流沉积型与矽卡岩型矿床的争论。文章针对该争论,通过对永平 Cu-W 矿床的白钨矿开展微量元素分析,研究了成矿流体性质、来源和矿床成因。永平 Cu-W 矿床发育 3 种类型白钨矿:退化蚀变阶段暗色均质白钨矿Ⅰ-1;亮色均质白钨矿Ⅰ-2;石英-硫化物阶段具有环带结构的白钨矿Ⅱ。白钨矿中 Mo 含量和 Eu 异常能够指示成矿流体氧化还原性。白钨矿Ⅰ-1 富集 Mo 元素,并呈负 Eu 异常,指示氧化性;白钨矿Ⅰ-2 和白钨矿Ⅱ中 Mo 含量减少,并且呈正 Eu 异常,指示成矿流体的氧逸度降低。永平 Cu-W 矿床所有白钨矿均呈明显的轻稀土元素富集模式,与典型矽卡岩型白钨矿稀土元素特征相一致,而明显不同于石英脉型矿床白钨矿中稀土元素或重稀土元素富集模式。白钨矿具有高 Mo 和低 Sr 元素,与岩浆-热液白钨矿特征一致,而明显不同于变质来源的白钨矿,指示成矿流体来源于岩浆。白钨矿的 Y/Ho 比值范围为 19~43,与似斑状黑云母花岗岩（Y/Ho=25~30）相似,明显不同于石炭系叶家湾组（Y/Ho=34~75）,指示成矿流体主要来源于岩浆。 白钨矿地球化学特征指示永平 Cu-W 矿床为矽卡岩型矿床。

关键词 地球化学;白钨矿;微量元素;矿床成因;永平 Cu-W 矿床

中图分类号:P618.41;P618.67 **文献标志码**:A

Trace element geochemistry of scheelites from Yongping Cu-W deposit in Jiangxi: Implications for ore genesis

SU QiangWei[1], MAO JingWen[1], SONG ShiWei[1] and WANG XunJun[2]

(1 MNR Key Laboratory of Metallogeny and Mineral Assessment, Institute of Mineral Resources, Chinese Academy of Geological Sciences, Beijing 100037, China; 2 Geological Exploration Engineering Co., Ltd., Jiangxi Copper Group, Shangrao 334506, Jiangxi, China)

Abstract

The Yongping deposit is a large-sized Cu-W deposit in the Qin-Hang metallogenic belt. The ore genesis of submarine exhalative sedimentary versus skarn types has been debated for a long time. The trace element concentrations of scheelite from the Yongping deposit were analyzed for constraining mineralization conditions and the genesis. There are three types of scheelite from the Yongping deposit: (1) homogeneous scheelite with dark shade in CL image from retrograde alteration stage (Sch Ⅰ-1); (2) homogeneous scheelite with light shade in CL image from retrograde alteration stage (Sch Ⅰ-2); and (3) scheelite with oscillatory zoning from the quartz-sulfide stage (Sch Ⅱ). Mo and Eu substitution is of particular relevance, and shows redox sensitivity. The Sch Ⅰ-1 is Mo en-

* 本文得到国家自然科学基金项目(编号: 41820104010)和(编号: 41925011)联合资助

第一作者简介 苏蔷薇,女,1989 年生,博士研究生,矿床学专业,从事矿床学研究。Email: suqiangwei1@163.com

收稿日期 2020-07-03;改回日期 2020-07-28。张绮玲编辑。

riched and shows negative Eu anomaly, indicating an oxidized fluid, whereas the Sch Ⅰ-2 and Sch Ⅱ are Mo depleted and show positive Eu anomaly, indicating a reduced fluid. All scheelites from the Yongping deposit have relative LREE-enriched chrondrite-nomalized rare earth element patterns, which are consistent with those from the skarn deposits but are different from those in metamorphic deposits. The high values of Mo and low values of Sr in scheelite suggest a magmatic-hydrothermal origin instead of metamorphic origin. The similarity in Y/Ho ratios between scheelites and granite indicates that the ore-forming fluid was derived from the granite. In summary, these data strongly support that the Yongping deposit is a skarn-type deposit.

Key words: geochemistry, scheelite, trace element, ore genesis, Yongping deposit

钦杭成矿带是华南地区重要的中生代斑岩-矽卡岩Cu多金属成矿带(Mao et al., 2011a; 2013; 2014; Sun et al., 2011),其中发育一系列大型-超大型Cu多金属矿床,如德兴、永平、银山、东乡和圆珠顶等矿床(Mao et al., 2011b; Wang et al., 2013; Cai et al., 2016; Yuan et al., 2018)。江西永平矿床是钦杭成矿带东部一个重要的大型Cu-W矿床(铜金属量为1.75 Mt,平均品位为0.69%;WO_3金属量为0.13 Mt,平均品位为0.15%)。然而,永平矿床的成因一直是争论的焦点。有些学者认为永平Cu-W矿床与海底喷流沉积作用有关,并经后期热液叠加改造,主要依据是永平矿体沿着地层顺层产出,并且矿石具有层状、纹层状构造特征(徐克勤等,1996;赵常胜,2001;Gu et al., 2007)。而有些学者认为该矿床为与燕山期岩浆作用有关的斑岩Mo-矽卡岩Cu-W多金属矿床系列(毛景文等,2009;Ni et al., 2017),主要依据是永平似层状矿体与十字头岩体和矽卡岩蚀变具有密切的空间和时间关系,似层状Cu-W矿体中黄铁矿的Pb-Pb年龄为159 Ma(Zhu et al., 2016),与斑岩Mo矿辉钼矿的Re-Os年龄(158 Ma,李晓峰等,2007)和十字头岩体的锆石U-Pb年龄(160 Ma,Zhang et al., 2018)相一致。不同的成因模式指示不同的金属富集机制和适用不同的矿产勘查方案(Mao et al., 2011a; Li et al., 2018)。

白钨矿广泛分布在斑岩-矽卡岩钨矿床、石英脉型钨矿床及一些变质金矿床中。其在热液环境形成过程中,REE和Sr能够置换白钨矿($CaWO_4$)晶格中的Ca,从而在白钨矿中具有较高的含量(Brugger et al., 2000)。因此,白钨矿的REE可以用来约束成矿流体来源、流体的物理和化学性质(Brugger et al., 2000; Dostal et al., 2009; Ghaderi et al., 1999)。白钨矿中Eu异常、Mo和Sr含量能够记录成矿流体的氧化还原性质和水岩反应强度(Hsu et al., 1973; Ghaderi et al., 1999; Sun et al., 2017)。由于白钨矿的稀土元素和微量元素组成可以提供有关岩浆熔体和成矿流体的信息(Cottrant, 1981),不同的稀土元素模式和微量元素组成表明不同的物质来源和成矿条件(Tomschi et al., 1986)。进而解释矿床成因和指导矿床勘查(Song et al., 2014; Poulin et al., 2018; Sciuba et al. 2019)。如,石英脉型矿床中形成的白钨矿,其稀土元素具有中稀土元素(MREE)富集的特征(Ghaderi et al. 1999),矽卡岩型矿床白钨矿稀土元素具有重稀土元素亏损的特征(Song et al., 2014);岩浆热液环境形成的白钨矿具有更低的Sr/Mo比值(<10),变质环境形成的白钨矿具有更高的Sr/Mo比值(>10;Poulin et al., 2018)。永平Cu-W矿床中,白钨矿在矽卡岩矿石和块状矿石中普遍发育。白钨矿作为该矿床的主要矿石矿物,是示踪成矿流体的来源和演化,进而揭示矿床成因的理想研究对象。

1 区域地质及矿床地质特征

钦杭成矿带是华南地区重要的板内铜多金属成矿带(毛景文等,2008;2011)。钦杭成矿带在大地构造位置上处于扬子克拉通与华夏地块之间的新元古代碰撞拼接带(图1,Chen et al., 1998; Li et al., 2002)。扬子克拉通与华夏地块碰撞对接后,形成华南板块,随后经历了加里东期、印支期和燕山期多次构造岩浆活动(舒良树,2012)。至中-晚侏罗世,古太平洋板块向北西向俯冲至欧亚板块之下,引发大规模花岗质岩浆侵位和相关的Cu多金属矿床的形成,其成岩成矿时间在175~155 Ma之间(Mao et al., 2011a, 2013; Sun et al., 2011; Xie et al., 2011)。钱塘江-信江断裂拗陷带,裂凹陷带延长近800 km,宽度一般为60~100 km,其两侧均以深断裂为界,拗陷带的西北面是扬子地块,东南面则为华夏地块(倪培等,2005)。钦杭成矿带东北部基底地层为新

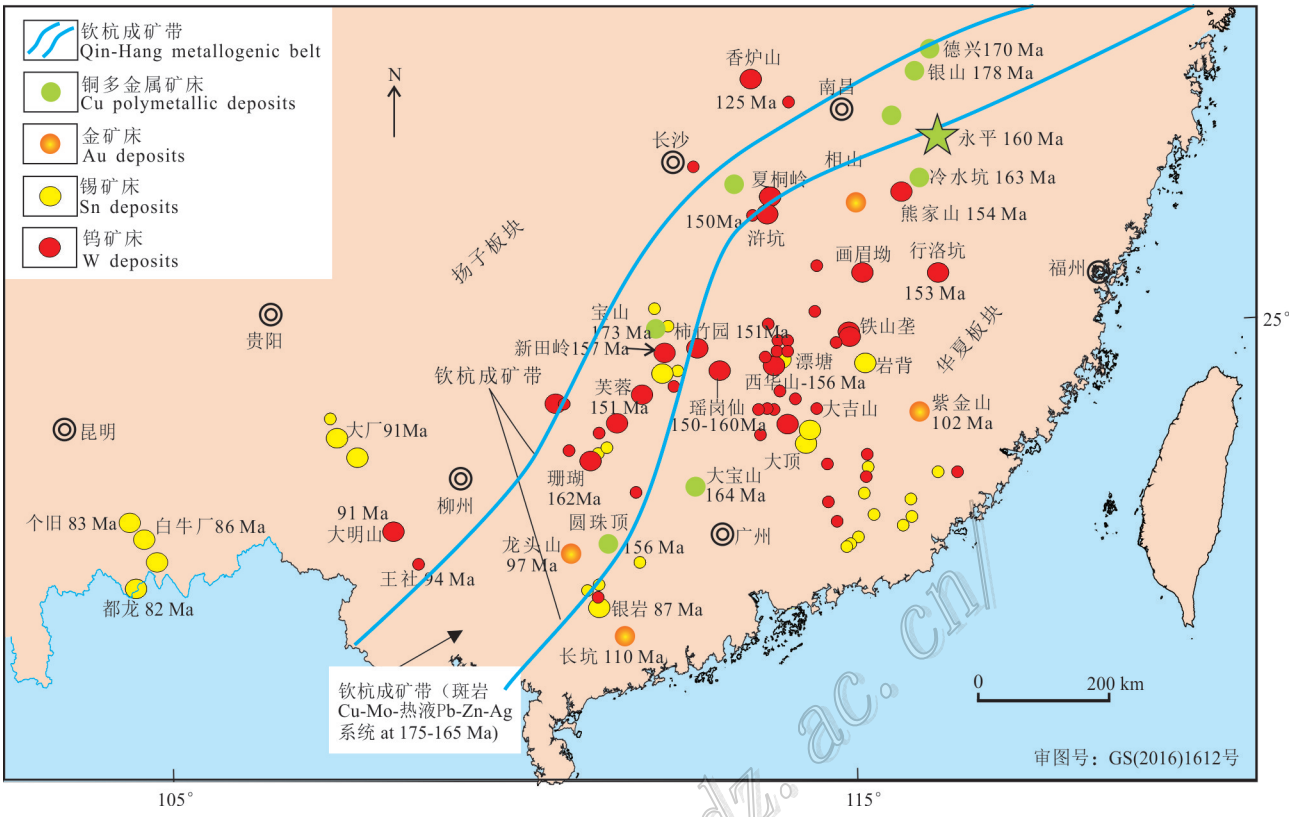

图 1　华南铜钨多金属矿床分布图 (据毛景文等,2011)

Fig. 1　Map showing the distribution of Cu-W polymetallic ore deposits in South China (after Mao et al., 2011)

元古界双桥山群和周潭群变质沉积岩夹铁镁质火山岩。盖层由寒武系—志留系碎屑岩、中泥盆统—下三叠统碳酸盐岩、中三叠统—下侏罗统海相陆源碎屑岩和早白垩世北东向伸展盆地中分布的火山岩组成(Zhu et al., 2016)。区域上岩浆活动以燕山期为主,燕山期岩体可以划分为 2 个阶段:175~155 Ma 和 144~121 Ma。第一阶段侵入岩体,以德兴铜厂、十字头岩体为代表,岩性为高钾钙碱性花岗闪长岩、黑云母花岗岩等。第二阶段侵入岩以冷水坑、灵山-三清山岩体为代表,岩性以碱性花岗岩为主(田明君等,2019)。

永平 Cu-W 矿床位于钦杭成矿带的东段(图 1)。矿区出露地层为新元古界周潭群变质沉积岩夹铁镁质火山岩,石炭系叶家湾组灰岩和砂岩、船山组灰岩、二叠系茅口组灰岩、李家组页岩(图 2a)。叶家湾组是矿区主要的赋矿地层。矿区主要构造有 NNE 向 F1 断裂和打字坪倒转向斜(图 2a)。永平矿体位于 F1 断裂的下盘和打字坪向斜的西翼。矿区岩浆活动发育,矿区东南部主要出露十字头-火烧岗似斑状黑云母花岗岩,矿区中部和西部主要出露一些石英斑岩脉和花岗斑岩脉(图 2a)。十字头岩体出露面积为 0.65 km^2,沿着近南北向断裂带侵位,呈不规则岩株状侵入到周潭群变质沉积岩和叶家湾组灰岩和砂岩中,与永平 Cu-W 矿床形成关系密切(图 2a)。石英斑岩沿近南北向断裂带展布,呈脉状侵入到周潭群变质沉积岩和叶家湾组灰岩和砂岩中,并穿切永平 Cu-W 矿体(图 2a)。花岗斑岩沿着近南北向断裂带分布,呈脉状侵入到周潭群变质沉积岩和叶家湾组灰岩和砂岩中,并穿切石英斑岩和永平 Cu-W 矿体(图 2a、b)。似斑状黑云母花岗岩、石英斑岩和花岗斑岩 LA-ICP-MS 锆石 U-Pb 年龄分别为(160.2±1.6)Ma、(158.7±1.5)Ma 和(152.7±1.7)Ma(Zhang et al., 2018)。矿区共有 7 个矿带,Ⅰ~Ⅵ矿带以 Cu-W 矿体为主,Ⅶ矿带是表生矿体。其中矿带Ⅱ是矿区最重要的成矿带,铜金属量占全区 72% 以上。该矿带内 Cu-W 矿体赋存于石炭系叶家湾组地层中,并且受断层 F1 的控制(图 2b)。该矿带内矿体主要以似层状产出,走向近南北向,倾向东,倾角 20°~50°。并

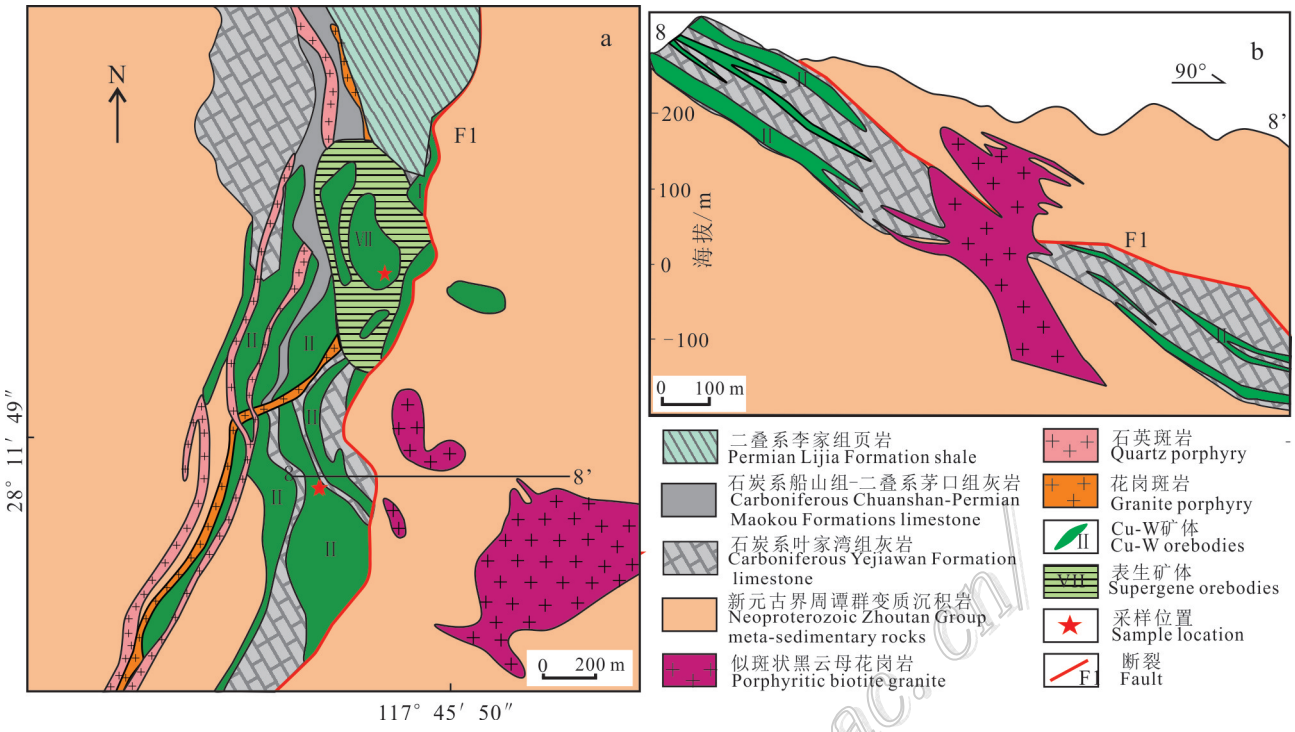

图2 永平Cu-W矿床地质简图(a)和8号勘探线剖面图(b)(据余祖寿等,2016)

Fig. 2 Geological map (a) and cross section along No. 8 exploration line (b) of the Yongping copper-tungsten deposit (after Yu et al., 2016)

且矿体规模大,沿走向最长2500 m,平均厚15.05 m,最大延伸至−670 m(陈军军等,2016)。矿区铜的平均品位为0.69%,WO_3平均品位为0.15%(余祖寿等,2016)。

永平Cu-W矿床中矿石类型以矽卡岩型矿石为主,矿石结构以交代结构为主。矿石构造主要有浸染状、脉状、块状构造等。矽卡岩以典型钙质硅酸盐矿物(石榴子石和透辉石)为主,含有少量退化蚀变矿物(绿帘石、透闪石、阳起石、绿泥石、石英、萤石和方解石),主要矿石矿物为黄铜矿、白钨矿、黄铁矿、磁黄铁矿、闪锌矿和方铅矿。热液蚀变作用主要为矽卡岩化、绿泥石化、硅化和碳酸盐化。根据野外调查和岩相学观察,划分为4个热液阶段:① 矽卡岩阶段;② 退化蚀变阶段;③ 石英-硫化物阶段;④ 碳酸盐阶段。矽卡岩阶段以大量钙质硅酸盐矿物沉淀(如石榴子石和辉石)为特征(图3a~c),石榴子石呈半自形-他形,具有环带结构(图4a)。退化蚀变阶段以含水硅酸盐矿物如绿帘石和绿泥石沉淀为特征(图3d),这些矿物通常与铜钨矿化相关。硫化物通常呈浸染状交代石榴子石和绿泥石(图4b)。硫化物主要为黄铜矿和黄铁矿(图4d),并且与白钨矿共生组合(图4c)。石英-硫化物阶段,以大量硫化物、白钨矿、石英和方解石为主,以富白钨矿和硫化物的石英脉穿切早期矽卡岩型矿石和围岩(图3e~g)为特征,该阶段是钨铜矿形成的重要阶段。硫化物主要为黄铜矿、闪锌矿、方铅矿,并且这些硫化物交代白钨矿(图3g~i)。碳酸盐阶段以贫矿方解石脉为主,这些方解石脉穿切围岩和石英-硫化物脉(图3i)。

2 样品采集及测试方法

用于分析石榴子石、绿帘石和白钨矿显微结构、微量元素的样品采自于矿区地表和钻孔中Cu-W矿体(图2)。样品的矿物学特征和采样位置列于表1。采用光学显微镜和扫描电子显微镜阴极发光仪观察白钨矿的物理性质,如形态、大小和颜色。采用LA-ICP-MS技术对选出的白钨矿颗粒进行微量元素地球化学特征进行分析。

本次研究采用了扫描电子显微镜阴极发光仪

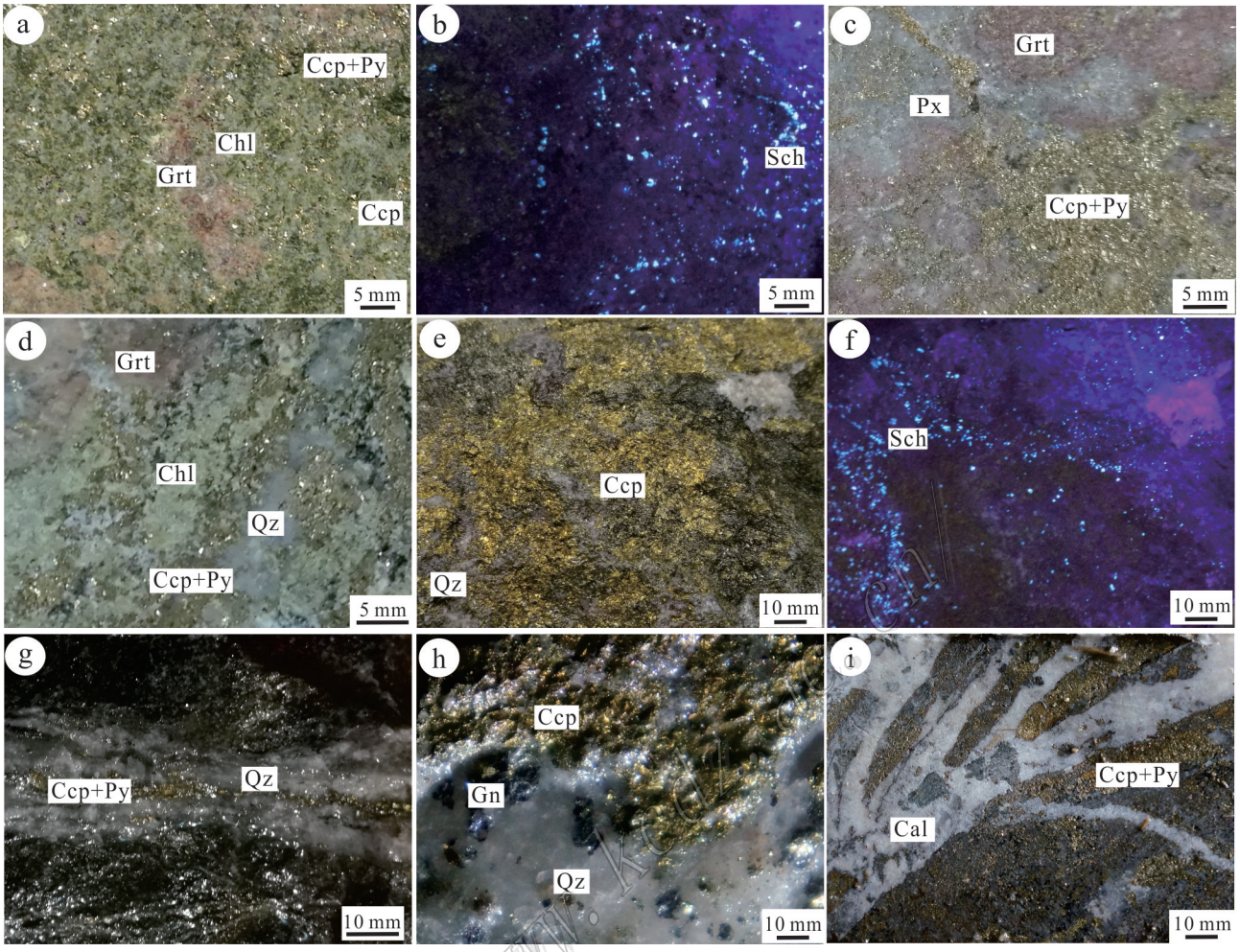

图 3　永平矿床 Cu-W 矿石照片

a. 浸染状矽卡岩铜矿石;b. 紫外线下浸染状白钨矿矿化矽卡岩型矿石;c. 石榴子石和辉石矽卡岩;d. 退化蚀变矽卡岩铜矿石;e. 块状铜矿石;f. 紫外线下含浸染状白钨矿矿化块状铜矿石;g. 石英-硫化物脉;h. 石英-硫化物脉;i. 方解石脉切穿块状铜矿石

Grt—石榴子石;Px—辉石;Chl—绿泥石;Ccp—黄铜矿;Qz—石英;Sch—白钨矿;Gn—方铅矿;Cal—方解石

Fig. 3　Photographs of copper-tungsten ores from the Yongping deposit

a. Garnet skarn with disseminated chalcopyrite; b. Garnet skarn with disseminated scheelite under ultraviolet light; c. Garnet and pyroxene skarn; d. Retrograde alteration skarn with disseminated chalcopyrite; e. Massive copper ore; f. Massive copper ore containing disseminated scheelite with blue luminescence under ultraviolet light; g. Quartz-sulfide vein containing chalcopyrite and scheelite; h. Massive copper ore containing chalcopyrite and galena; i. Calcite vein cutting copper ore

Grt—Garnet; Px—Pyroxene; Chl—Chlorite; Ccp—Chalcopyrite; Sch—Scheelite; Gn—Galena; Qz—Quartz; Cal—Calcite

(SEM-CL)观察白钨矿的显微结构。实验在中国地质科学院地质所完成,所使用的仪器为 FEI Nova NanoSEM 450 型号的扫面电子显微镜和 Gatan MonoCL 4 型号的阴极发光系统。为了对比不同白钨矿颗粒的阴极发光差异,对每种类型的样品的分析均是在相同的条件下。各项仪器的参数如下:使用电压为 10 kV,温度为室温(约 25℃),且每 1 张 CL 图像的采集时间均为 40 s。

石榴子石、绿帘石、白钨矿原位微量元素分析在国家地质实验测试中心完成,所用仪器为连接 New Wave 213 激光剥蚀系统的 Thermo Element Ⅱ 型质谱仪。激光剥蚀束斑直径为 40 μm,可控激光能量 23~25 J/cm^2,采集时间为 90 s,以 He 为载气,流量为 0.8 L/min。激光剥蚀方式为单点方式,激光器工作频率为 10 Hz。样品微量元素校正以 ^{44}Ca 为内标,以国际微量元素标样 NIST610、612

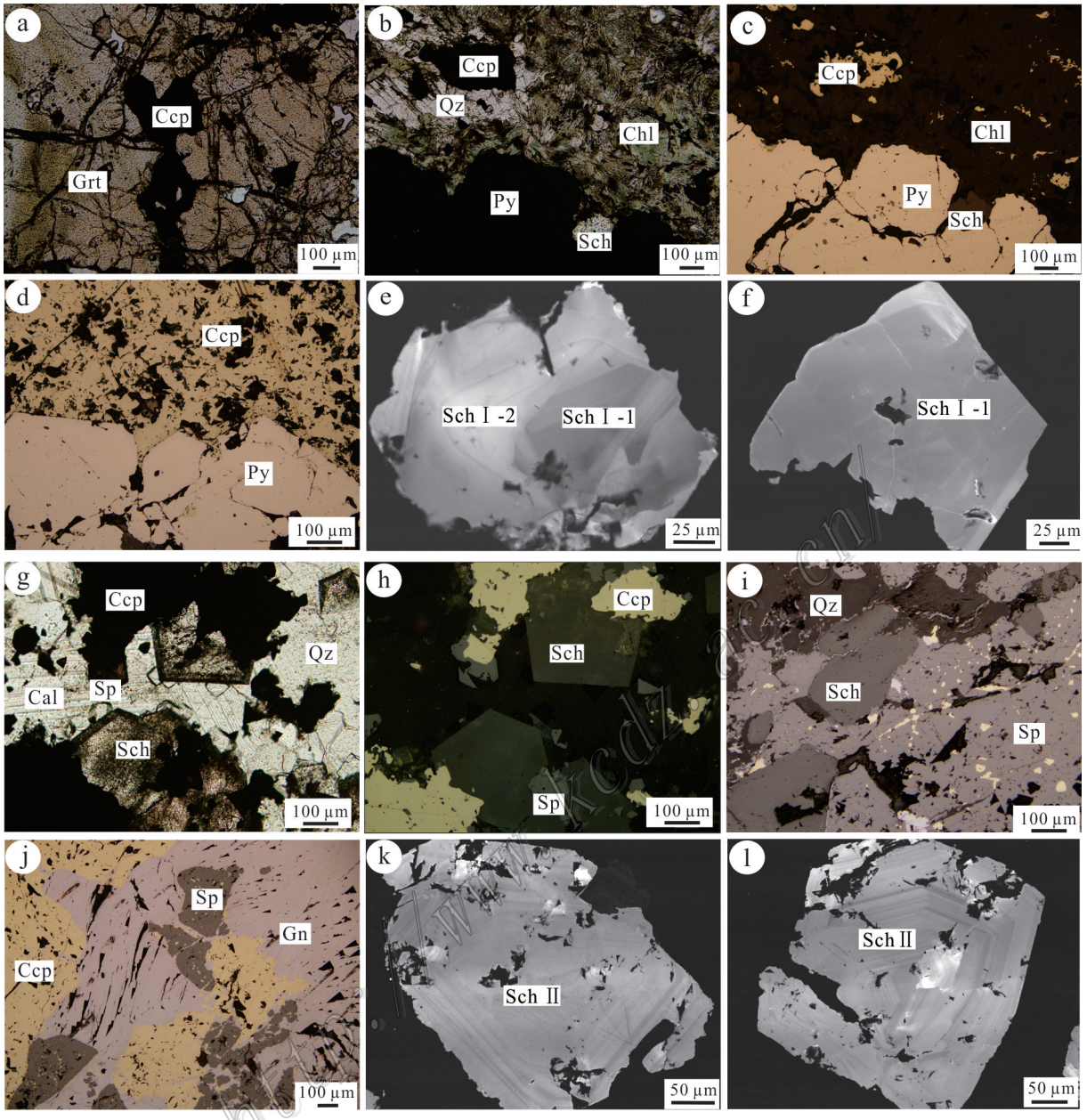

图4 永平Cu-W矿床白钨矿显微镜下及阴极发光照片

a. 黄铜矿交代石榴子石(单偏光);b. 白钨矿Ⅰ与绿泥石、石英、黄铜矿、黄铁矿共生(单偏光);c. 黄铜矿和黄铁矿与白钨矿Ⅰ共生(反射光);d. 黄铜矿和黄铁矿共生(反射光);e. 白钨矿核边结构,边部白钨矿Ⅰ-2和核部白钨矿Ⅰ-1(阴极发光);f. 白钨矿Ⅰ-1均一结构(阴极发光);g、h. 黄铜矿和闪锌矿交代白钨矿Ⅱ(单偏光和反射光);i. 闪锌矿叠加沉淀在白钨矿Ⅱ周围(反射光);j. 黄铜矿、闪锌矿、方铅矿共生(反射光);k、l. 白钨矿Ⅱ具有环带结构(阴极发光)

Grt—石榴子石;Chl—绿泥石;Ccp—黄铜矿;Py—黄铁矿;Qz—石英;Sch Ⅰ-1—白钨矿Ⅰ-1;Sch Ⅰ-2—白钨矿Ⅰ-2;Sch Ⅱ—白钨矿Ⅱ;Sp—闪锌矿;Gn—方铅矿;Cal—方解石

Fig. 4 Microphotograph and cathodoluminescence (CL) images of scheelites from the Yongping deposit

a. Garnet crosscut by chalcopyrite with transmitted light; b. Scheelite Ⅰ coexisting with chlorite, quartz, chalcopyrite and pyrrhotite with transmitted light; c. Scheelite Ⅰ coexisting with chalcopyrite and pyrrhotite with reflected light; d. Chalcopyrite-pyrrhotite assemblage with reflected light; e. CL images of scheelite Ⅰ-1 overgrowth by scheelite Ⅰ-2; f. CL images of scheelite Ⅰ-1 with homogeneous texture; g,h Scheelite Ⅱ replaced by chalcopyrite and sphalerite with transmitted light and reflected light; i. Scheelite Ⅱ coexisting with sphalerite with reflected light; j. Chalcopyrite-sphalerite-galena assemblage with reflected light; k,l. CL images of scheelite Ⅱ with oscillatory growth zoning

Grt—Garnet; Chl—Chlorite; Sch—Scheelite; Ccp—Chalcopyrite; Py—Pyrite; Sp—Sphalerite; Gn—Galena; Qz—Quartz; Cal—Calcite

表1　永平矿床样品描述和采样位置

Table 1　Details of scheelite samples from the Yongping deposit

样品编号	采样位置	样品描述
15XY-12	113 m, ZK205	矽卡岩阶段,白钨矿与石榴子石、绿帘石、黄铜矿、磁黄铁矿、石英矿物组合
15XY-14	141 m, ZK205	矽卡岩阶段,白钨矿与石榴子石、绿泥石、黄铜矿、磁黄铁矿、石英矿物组合
15XY-15	146 m, ZK205	矽卡岩阶段,白钨矿与石榴子石、绿泥石、黄铜矿、磁黄铁矿、石英矿物组合
YP-2	117°45′41″, 28°11′44″	石英-硫化物阶段,白钨矿与黄铜矿、闪锌矿、方铅矿、石英、方解石矿物组合
YP2-2	117°45′41″, 28°11′44″	石英-硫化物阶段,白钨矿与黄铜矿、闪锌矿、方铅矿、石英、方解石矿物组合
YP-10	117°45′43″, 28°12′7″	石英-硫化物阶段,白钨矿与黄铜矿、闪锌矿、方铅矿、石英、方解石矿物组合

为外标计算得来。检测限见表2和表3。

3　测试结果

3.1　白钨矿结构特征

根据阴极发光(CL)结构特征和矿物共生组合,划分出3种类型白钨矿,退化蚀变阶段暗色均质白钨矿Ⅰ-1和亮色均质白钨矿Ⅰ-2,石英-硫化物阶段具有环带结构白钨矿Ⅱ。白钨矿Ⅰ呈浸染状分布在矽卡岩矿石中(图3a),并且在短波紫外线下呈黄色荧光(图3b)。白钨矿Ⅰ呈半自形-他形,颗粒直径大小在0.1~0.3 mm之间,通常与绿泥石、透闪石、绿帘石、硫化物和石英共生(图4b、c)。白钨矿Ⅰ在阴极发光图像中多呈现暗色均质结构,另有少部分显示核边结构(图4f)。边部(白钨矿Ⅰ-2)显示亮色均质结构,核部(白钨矿Ⅰ-1)显示暗色均质结构(图4e)。

白钨矿Ⅱ出现在富硫化物的石英脉中,并且在短波紫外线下呈蓝色荧光(图3f)。白钨矿Ⅱ呈半自形-他形,颗粒直径大小为0.2~0.5 mm,通常与大量硫化物(黄铜矿、闪锌矿、方铅矿)、石英和方解石关系密切(图4g~i),可见白钨矿Ⅱ被黄铜矿和闪锌矿交代(图4h、i)。CL图像显示白钨矿Ⅱ具有明显的震荡环带结构,生长环带宽度在1~30 μm之间(图4k、l)。

3.2　微量元素地球化学

永平Cu-W矿床石榴子石、绿帘石和3种类型白钨矿的LA-ICP-MS微量元素分析结果见表2和表3,球粒陨石标准化稀土元素配分模式见图5。

石榴子石稀土元素球粒陨石标准化配分曲线显示重稀土元素富集(图5a),LREE/HREE比值在0.54~1.52之间,w(ΣREE)为20.8×10^{-6}~28.2×10^{-6},Eu/Eu*比值在0.35~0.78范围(表2)。另外,石榴子石w(W)为1.66×10^{-6}~9.23×10^{-6},w(S)为186×10^{-6}~1048×10^{-6},w(Y)为10.7×10^{-6}~26.5×10^{-6}(表3)。绿帘石稀土元素球粒陨石标准化配分曲线显示相对轻稀土元素富集(图5b),LREE/HREE比值在7.3~27.1范围,w(REE)为136.2×10^{-6}~837.1×10^{-6},Eu/Eu*比值为1.32~2.56。另外,绿帘石的w(W)、w(S)、w(Sr)和w(Y)分别在2×10^{-6}~5425×10^{-6}、0~9378×10^{-6}、747×10^{-6}~1031×10^{-6}和17.8×10^{-6}~35.0×10^{-6}之间。

白钨矿Ⅰ-1稀土元素球粒陨石标准化配分曲线显示典型的右倾模式(图5a),LREE/HREE比值在3.0~13.6之间,w(ΣREE)为109.3×10^{-6}~2134.2×10^{-6},Eu/Eu*比值在0.60~1.33范围。另外,白钨矿Ⅰ-1中w(Mo)为$15\ 280\times10^{-6}$~$28\ 860\times10^{-6}$,w(Cu)为154×10^{-6}~7228×10^{-6},w(S)为2400×10^{-6}~$10\ 051\times10^{-6}$,w(Sr)为26.4×10^{-6}~45.1×10^{-6},w(Y)为30.5×10^{-6}~160.8×10^{-6}(表3)。与白钨矿Ⅰ-1比较,白钨矿Ⅰ-2的稀土元素球粒陨石标准化配分曲线显示相同的右倾模式(图5b),LREE/HREE比值在3.0~24.3之间,w(ΣREE)为648.0×10^{-6}~3182.5×10^{-6},Eu/Eu*比值在1.52~3.51范围。白钨矿Ⅰ-2中w(Mo)为238×10^{-6}~1735×10^{-6},w(S)为0~304×10^{-6},w(Sr)为28.7×10^{-6}~247.4×10^{-6},w(Y)为55.5×10^{-6}~246.0×10^{-6}。白钨矿Ⅱ稀土元素球粒陨石标准化配分曲线显示轻稀土元素富集模式(图5c),LREE/HREE比值在3.8~19.0之间,w(ΣREE)为243.6×10^{-6}~1023.5×10^{-6},Eu/Eu*比值在1.79~17.88范围。另外,白钨矿Ⅱ中w(Mo)为69×10^{-6}~1469×10^{-6},w(S)为0~398×10^{-6},w(Sr)为28.8×10^{-6}~144.0×10^{-6},w(Y)为33.4×10^{-6}~290.2×10^{-6}。

4　讨　论

4.1　成矿流体性质

白钨矿晶体中Mo元素含量能够用于指示成矿流体的氧化还原性(Hsu et al., 1973; Linnen et al.,

表2 永平矿床白钨矿、石榴子石、绿帘石稀土元素含量

Table 2 Rare element compositions of scheelite, garnet and epidote from the Yongping deposit

样品编号	矿物	w(B)/10^{-6}																LREE/HREE	δEu	Eu_N	Eu_N*
		La	Ce	Pr	Nd	Sm	Eu	Gd	Tb	Dy	Ho	Er	Tm	Yb	Lu	Y	ΣREE				
ZK-15-1	SchⅠ-1	292.340	1141.910	94.870	385.470	62.130	11.310	50.660	7.500	40.370	7.100	19.490	2.650	16.330	2.070	160.860	2134.200	13.600	0.600	153.890	257.100
ZK-15-2	SchⅠ-1	45.850	227.140	36.390	167.840	33.280	7.870	26.850	3.930	20.250	3.930	10.670	1.510	10.690	1.340	82.850	597.600	6.550	0.780	107.130	137.170
ZK-15-3	SchⅠ-1	13.460	54.380	8.680	43.280	10.720	2.860	8.360	1.260	7.110	1.350	3.160	0.330	2.280	0.250	30.470	157.500	5.530	0.890	38.890	43.620
ZK-15-4	SchⅠ-1	8.360	33.330	5.440	24.790	6.920	3.180	7.640	1.320	8.980	1.650	4.630	0.480	2.300	0.250	36.040	109.300	3.010	1.330	43.300	32.500
ZK-15-5	SchI-1	120.470	452.970	41.820	154.550	30.420	100	28.430	4.700	28.800	5.870	13.780	1.830	11.450	1.320	113.650	906.400	8.420	1.020	136.030	132.890
ZK-12-1	SchⅠ-2	42.330	156.260	29.370	167.780	53.310	65.500	60.810	7.380	36.080	6.500	13.910	1.420	6.430	0.910	181.390	648.000	3.860	3.510	891.220	254.090
ZK-12-2	SchⅠ-2	36.070	131.640	26.870	166.440	63.250	73.570	69.340	9.440	47.350	8.460	17.600	1.620	8.810	1.290	222.630	661.700	3.040	3.380	1000.940	296.040
ZK-12-3	SchⅠ-2	50.970	205.180	35.470	215.760	83.960	75.620	81.280	9.670	50.860	8.910	19.650	1.580	8.490	1.220	237.100	848.600	3.670	2.760	1028.880	372.190
ZK-12-4	SchⅠ-2	74.750	313.590	53.280	351.830	110.220	56.000	113.790	14.150	65.660	11.530	23.350	2.350	9.960	1.210	293.170	1201.700	3.970	1.520	761.870	502.290
ZK-12-5	SchⅠ-2	47.960	209.150	46.850	292.840	106.160	77.970	104.810	13.150	63.530	10.950	24.520	2.000	9.980	1.350	288.230	1011.200	3.390	2.230	1060.870	474.560
ZK-14-1	SchⅠ-2	155.170	825.220	104.490	515.440	124.650	67.460	105.030	14.220	72.500	12.420	28.640	3.230	17.440	1.950	366.230	2047.900	7.020	1.750	742.340	481.820
ZK-14-2	SchⅠ-2	345.090	1495.670	159.030	555.200	74.550	71.470	55.100	6.490	35.590	6.980	18.800	2.700	15.990	1.820	297.170	2844.500	18.820	3.260	864.040	589.520
ZK-14-3	SchⅠ-2	266.940	1234.710	145.660	547.000	79.740	56.680	58.640	6.970	34.170	6.600	19.000	2.410	12.830	1.570	265.900	2472.900	16.390	2.420	799.210	889.210
ZK-14-4	SchⅠ-2	293.950	1338.730	157.350	620.650	98.130	61.320	68.340	7.720	40.980	7.630	19.490	2.450	14.160	1.680	274.440	2732.600	15.820	2.170	898.440	529.220
ZK-14-5	SchⅠ-2	493.730	1742.370	161.680	527.800	70.150	60.930	49.920	6.230	31.170	6.130	16.450	2.180	12.170	1.610	238.630	3182.500	24.290	3.000	902.200	598.380
ZK-15-6	SchⅠ-2	241.630	1319.140	165.110	660.250	98.590	51.870	77.030	9.210	42.210	8.090	22.220	2.430	15.340	1.890	292.070	2715.000	14.220	1.760	257.970	77.140
ZK-15-7	SchⅠ-2	237.060	1089.340	124.850	474.140	73.020	57.390	52.880	6.190	32.520	6.330	16.840	2.190	11.730	1.540	255.960	2186.000	15.790	2.690	276.990	65.580
ZK-15-8	SchⅠ-2	238.970	1132.220	142.170	495.170	71.430	57.740	55.130	5.950	33.300	5.910	17.420	2.140	11.870	1.380	251.250	2270.800	16.060	2.710	267.450	37.600
YP2-2-1	SchⅡ	101.010	272.480	43.360	197.880	41.440	25.160	39.140	6.060	38.510	8.160	20.010	2.320	16.320	2.260	277.170	814.100	5.130	1.880	337.570	75.530
YP2-2-2	SchⅡ	107.980	259.560	49.230	211.950	42.800	26.760	41.320	6.060	39.590	8.070	22.060	3.040	18.180	2.140	290.180	838.700	4.970	1.920	257.610	41.970
YP2-2-3	SchⅡ	44.590	109.390	18.170	85.800	19.280	21.990	20.600	3.360	21.160	4.390	11.350	1.450	8.890	1.190	156.270	371.600	4.130	3.350	334.430	36.380
YP2-2-4	SchⅡ	52.930	134.590	25.120	113.570	27.550	29.290	30.350	4.160	28.170	5.930	15.480	1.990	12.610	1.820	209.450	483.600	3.810	3.080	154.350	54.620
YP2-2-5	SchⅡ	40.960	104.430	20.120	91.060	22.250	22.210	21.410	3.280	19.430	3.790	10.300	1.280	9.280	1.180	141.190	371.000	4.300	3.070	211.900	36.910
YP2-2-6	SchⅡ	40.090	96.830	16.830	76.440	16.760	18.960	17.690	2.840	16.530	3.190	8.750	1.020	7.670	0.930	106.690	324.500	4.540	3.340	425.020	45.360
YP2-2-7	SchⅡ	30.610	80.960	16.010	62.630	13.960	20.360	15.430	2.380	14.150	2.830	8.240	1.030	6.540	0.910	96.680	276.100	4.360	4.220	403.480	35.290

续表 2

Continued Table 2

样品编号	矿物	$w(B)/10^{-6}$																LREE/HREE	δEu	Eu_N	Eu_N*
		La	Ce	Pr	Nd	Sm	Eu	Gd	Tb	Dy	Ho	Er	Tm	Yb	Lu	Y	ΣREE				
YP-2-1	SchⅡ	101.220	199.990	22.740	62.710	8.840	29.660	6.550	0.850	5.280	0.960	2.660	0.580	4.930	0.560	42.230	447.500	19.020	11.410	288.320	26.760
YP-2-2	SchⅡ	73.780	132.290	15.070	43.410	6.680	21.190	4.980	0.920	4.830	1.010	2.660	0.430	3.290	0.370	33.410	310.900	15.810	10.760	528.500	29.520
YP-2-3	SchⅡ	75.370	147.540	15.760	49.670	7.180	38.840	5.760	0.870	5.690	1.230	4.050	0.700	6.690	1.150	34.770	360.500	12.790	17.880	153.600	85.510
YP-2-4	SchⅡ	35.480	111.400	19.090	79.840	20.920	11.290	16.510	2.380	12.260	2.430	6.100	0.840	4.160	0.720	77.490	323.400	6.120	1.790	284.450	76.770
YP-2-5	SchⅡ	86.040	256.330	35.980	128.310	19.300	20.910	14.130	2.150	10.710	2.310	6.230	0.860	5.290	0.670	73.350	589.200	12.910	3.700	378.000	123.380
YP-2-6	SchⅡ	139.970	494.480	64.410	207.660	30.700	27.780	23.140	2.620	14.340	2.630	7.810	1.010	6.060	0.920	107.150	1023.500	16.490	3.060	425.760	110.110
YP-2-7	SchⅡ	136.000	408.170	50.070	179.250	27.240	31.290	20.860	3.120	18.010	3.300	9.750	1.540	10.190	1.260	118.440	900.100	12.230	3.860	601.130	54.430
YP-2-8	SchⅡ	53.540	132.640	20.020	68.030	12.880	44.180	11.090	1.660	9.590	2.400	5.990	0.780	9.860	1.330	56.160	374.000	7.760	11.030	917.850	522.370
YP-10-1	SchⅡ	88.540	183.750	22.700	65.260	10.840	25.320	7.410	0.970	6.700	1.400	4.440	0.770	5.850	0.870	49.210	424.800	13.950	8.170	972.320	297.520
YP-10-2	SchⅡ	53.660	131.660	17.480	58.590	8.680	19.660	7.940	1.430	8.410	1.450	4.600	0.720	5.130	0.650	54.110	320.100	9.550	7.100	771.160	317.650
YP-10-3	SchⅡ	65.530	170.100	24.640	93.640	18.350	24.810	14.750	2.200	14.740	2.940	7.100	1.330	8.040	1.140	87.550	449.300	7.600	4.460	834.270	383.550
YP-10-4	SchⅡ	40.980	100.050	12.870	49.200	9.690	18.930	8.870	1.280	7.090	1.500	4.560	0.670	4.290	0.640	55.510	260.600	8.020	6.130	829.030	276.240
YP-10-5	SchⅡ	49.960	108.420	14.480	54.750	9.270	24.580	6.530	1.060	6.600	1.460	3.910	0.520	3.720	0.480	48.380	285.700	10.770	9.180	705.770	401.500
YP-10-6	SchⅡ	29.530	82.210	13.610	66.250	13.120	11.340	10.860	1.560	7.720	1.430	3.110	0.380	2.140	0.290	37.880	243.600	7.860	2.820	780.880	289.310
YP-10-7	SchⅡ	52.000	102.880	13.950	46.450	9.240	15.570	6.850	1.160	5.500	1.060	3.160	0.400	2.880	0.380	36.040	261.500	11.230	5.730	785.630	289.580
YP-10-8	SchⅡ	110.750	228.830	28.440	91.700	11.460	31.240	8.270	1.250	7.380	1.360	4.220	0.740	5.280	0.840	56.190	531.800	17.120	9.350	794.550	306.780
ZK-15-9	石榴子石	0.280	1.850	0.480	6.460	3.150	0.410	2.540	0.430	2.120	0.380	0.840	0.220	1.630	0.150	10.760	20.900	1.520	0.430		
ZK-15-10	石榴子石	0.080	1.110	0.370	3.680	2.130	0.580	2.920	0.510	3.090	0.880	2.340	0.320	2.490	0.290	19.380	20.800	0.620	0.710		
ZK-15-11	石榴子石	0.010	0.920	0.300	3.470	2.620	0.340	3.250	0.580	3.450	0.670	2.760	0.440	2.670	0.340	28.230	21.800	0.540	0.350		
ZK-15-12	石榴子石	5.730	9.650	2.240	6.490	2.100	0.650	3.120	0.910	4.280	0.950	4.140	0.290	4.130	0.640	26.500	45.300	1.460	0.780		
ZK-12-6	绿帘石	223.950	406.990	36.630	111.390	19.000	9.430	13.730	1.480	6.630	1.100	3.590	0.330	2.470	0.400	35.000	837.100	27.150	1.700		
ZK-12-7	绿帘石	35.520	69.300	7.890	28.120	7.350	3.020	6.580	0.840	5.130	1.150	2.560	0.520	3.400	0.450	31.400	171.800	7.330	1.300		
ZK-12-8	绿帘石	87.250	180.610	18.950	75.010	16.400	8.210	11.140	1.070	4.830	0.830	1.910	0.180	1.480	0.160	20.590	408.000	17.900	1.760		
ZK-12-9	绿帘石	30.450	58.760	5.890	20.030	6.160	2.330	4.260	0.570	3.190	0.700	1.780	0.180	1.670	0.240	17.850	136.200	9.810	1.320		
ZK-12-10	绿帘石	179.800	295.040	30.600	97.150	17.610	13.790	14.470	1.940	6.850	1.300	2.860	0.450	2.530	0.230	31.950	664.600	20.700	2.560		
检测限		0.100	0.060	0.040	0.280	0.340	0.090	0.360	0.030	0.100	0.020	0.060	0.020	0.120	0.020	0.160					

$Eu_N^*=(Sm_N+Gd_N)/2$

表3 永平矿床白钨矿、石榴子石、绿帘石微量元素含量

Table 3 Trace element compositions of scheelite, garnet and epidote from the Yongping deposit

样品编号	矿物	w(B)/%		w(B)/10^{-6}											
		Na_2O	CaO	W	Mo	Cu	S	Cr	As	Sr	Nb	Ta	Pb	Th	U
ZK-15-1	SchⅠ-1	0	18.10	645265.00	15280	154.00	10051	59.300	2.700	30.300	17.900	0.600	2.200	4.000	5.300
ZK-15-2	SchⅠ-1	0	19.48	627987.00	22902.00	7229.00	3782	1828.300	7.800	29.900	9.600	0.500	1.700	0.600	0.100
ZK-15-3	SchⅠ-1	0	19.42	636157.00	28861.00	1320	3002	27.700	1.700	28.700	3.300	0.500	3.100	0.200	0.100
ZK-15-4	SchⅠ-1	0	19.65	614082.00	20430	544.00	2400	587.800	11.400	26.400	6.100	0.300	481.100	0.200	0.200
ZK-15-5	SchⅠ-1	0	18.57	544196.00	15290	1031.00	2661	1159.100	0.800	45.100	23.500	0.400	2.300	2.200	3.200
ZK-12-1	SchⅠ-2	0	19.56	632672.00	1514.00	0	304	56.000	14.900	246.000	1.800	0.500	6.400	0	0.100
ZK-12-2	SchⅠ-2	0	18.42	645194.00	270	0	0	44.200	4.900	60.400	1.300	0.500	16.400	0	0.100
ZK-12-3	SchⅠ-2	0	19.54	634615.00	835.00	0	0	278.700	4.900	65.200	1.400	0.400	194.400	0	0.100
ZK-12-4	SchⅠ-2	0	17.80	648456.00	239.00	0	0	458.400	5.600	56.100	2.500	0.600	6.400	0	0.100
ZK-12-5	SchⅠ-2	0	17.99	647131.00	727.00	0	128	8.300	5.700	55.600	2.300	0.500	2.300	0	0
ZK-14-1	SchⅠ-2	0	19.38	634750	623.00	0	0	195.100	6.400	61.500	5.200	0.400	14.900	0	0.100
ZK-14-2	SchⅠ-2	0	19.83	630950	377.00	0	154	64.200	6.500	69.300	9.000	0.500	5.500	0	0.100
ZK-14-3	SchⅠ-2	0	19.49	632663.00	328.00	0	73	18.200	10.900	67.100	8.200	0.500	8.000	0	0.100
ZK-14-4	SchⅠ-2	0	20.21	624444.00	1440	0	241	41.700	14.900	74.000	8.700	0.500	25.900	0	0.100
ZK-14-5	SchⅠ-2	0	20.26	625212.00	1200	0	140	100.300	17.900	81.800	13.300	0.400	17.700	0.100	0.400
ZK-15-6	SchⅠ-2	0	18.34	642503.00	771.00	0	41	569.900	100	73.700	8.400	0.400	8.700	0.100	0.100
ZK-15-7	SchⅠ-2	0	20.71	621936.00	1736.00	0	40	394.500	18.400	79.300	7.100	0.500	23.000	0	0.100
ZK-15-8	SchⅠ-2	0	18.37	642505.00	652.00	0	146	207.000	9.900	67.300	8.000	0.400	9.400	0.100	0.100
YP2-2-1	SchⅡ	0	17.90	619219.00	264.00	0	398	432.700	8.500	28.800	5.000	0.500	1.800	4.200	48.000
YP2-2-2	SchⅡ	0	17.52	644049.00	286.00	0	0	240.900	10.300	31.200	5.000	0.400	1.800	5.700	43.800
YP2-2-3	SchⅡ	0	17.90	645464.00	342.00	0	118	232.200	4.500	45.500	5.400	0.500	1.800	3.700	28.200
YP2-2-4	SchⅡ	0	18.79	639230	291.00	0	41	51.400	22.600	46.400	4.700	0.400	2.000	3.400	22.200
YP2-2-5	SchⅡ	0	17.40	634124.00	482.00	0	0	120.200	6.400	42.100	5.900	0.400	1.700	3.100	27.100
YP2-2-6	SchⅡ	0	18.26	639196.00	329.00	0	0	556.200	2.300	52.200	3.300	0.400	2.700	3.000	13.600
YP2-2-7	SchⅡ	0	19.43	631767.00	396.00	0	145	332.100	4.200	45.100	2.600	0.400	1.600	1.900	4.500
YP-2-1	SchⅡ	0	19.79	633733.00	435.00	0	127	308.900	0	46.700	2.100	0.500	5.500	5.500	12.400
YP-2-2	SchⅡ	0	20.04	628952.00	674.00	0	69	1062.100	0	500	6.000	0.500	5.900	4.500	9.800
YP-2-3	SchⅡ	0	18.57	643744.00	293.00	0	71	114.700	0	64.000	1.800	0.400	5.500	10.700	19.300
YP-2-4	SchⅡ	0	18.38	645271.00	142.00	0	212	53.600	0	31.000	6.700	0.500	3.300	0.800	0.400
YP-2-5	SchⅡ	0	18.29	645152.00	653.00	0	291	546.000	0	33.100	3.500	0.500	3.300	1.800	10.300
YP-2-6	SchⅡ	0	20.41	628472.00	254.00	0	87	263.200	0	29.900	6.900	0.500	3.200	2.000	7.400
YP-2-7	SchⅡ	0	19.62	634656.00	70	0	221	200.900	0	38.700	4.700	0.500	4.100	2.600	8.200
YP-2-8	SchⅡ	0	19.41	621890	116.00	0	53	11559.700	0.200	76.000	2.500	0.500	6.900	10.200	11.400
YP-10-1	SchⅡ	0	18.17	645136.00	492.00	0	40	576.000	0	144.000	100	0.500	5.800	3.000	16.000
YP-10-2	SchⅡ	0.01	19.96	630872.00	537.00	0	48	398.300	0.500	40.200	11.700	0.700	4.000	3.600	4.800
YP-10-3	SchⅡ	0	19.92	630920	429.00	0	0	811.300	0	49.100	10.400	0.500	5.800	3.600	7.800
YP-10-4	SchⅡ	0	19.10	639207.00	638.00	0	25	411.200	0	45.800	12.300	0.600	5.100	2.300	6.600
YP-10-5	SchⅡ	0	20.57	626872.00	777.00	0	265	2000	0	39.100	3.800	0.600	3.800	1.000	6.200
YP-10-6	SchⅡ	0	18.48	644913.00	739.00	0	0	17.900	0	32.000	6.700	0.400	2.500	0.300	1.100
YP-10-7	SchⅡ	0	18.63	642757.00	1469.00	0	78	195.800	1.700	38.500	3.500	0.600	2.700	1.900	7.700
ZK-15-9	SchⅡ	0	37.62	2.00	1.00	1.00	813	13.700	3.200	0.300	7.800	1.200	0	0.100	0.900
ZK-15-10	石榴子石	0	39.55	5.00	0	7.00	1048	294.600	4.600	0.400	19.300	3.500	0.200	0.400	2.300
ZK-15-11	石榴子石	0	37.88	6.00	0	0	256	273.800	0	0.200	20.300	3.000	0.200	0.200	2.400
ZK-15-12	石榴子石	0	38.42	9.00	0	0	186	1145.800	1.600	9.400	23.800	2.200	6.800	1.800	4.500
ZK-12-6	绿帘石	0	24.57	48.00	1.00	9.00	0	336.400	22.700	1031.000	0.100	0	325.600	4.100	14.400
ZK-12-7	绿帘石	0	24.72	9.00	1.00	54.00	1857	2861.500	59.200	986.200	0.100	0	6186.400	0.100	8.100
ZK-12-8	绿帘石	0	23.96	2.00	0	10	878	575.900	16.700	747.600	0.100	0	1065.100	20.800	22.700
ZK-12-9	绿帘石	0.03	15.14	5.00	1.00	18.00	9379	2056.800	100.300	854.100	4.500	0.200	771.600	0.100	3.000
ZK-12-10	绿帘石	0	24.16	5424.00	0	9.00	501	4058.600	7.000	806.100	0.200	0	184.900	7.800	28.800
检测限		0.01	0.02	0.22	1.14	4.50	193	1.860	4.510	0.210	0.080	0.020	0.190	0.010	0.010

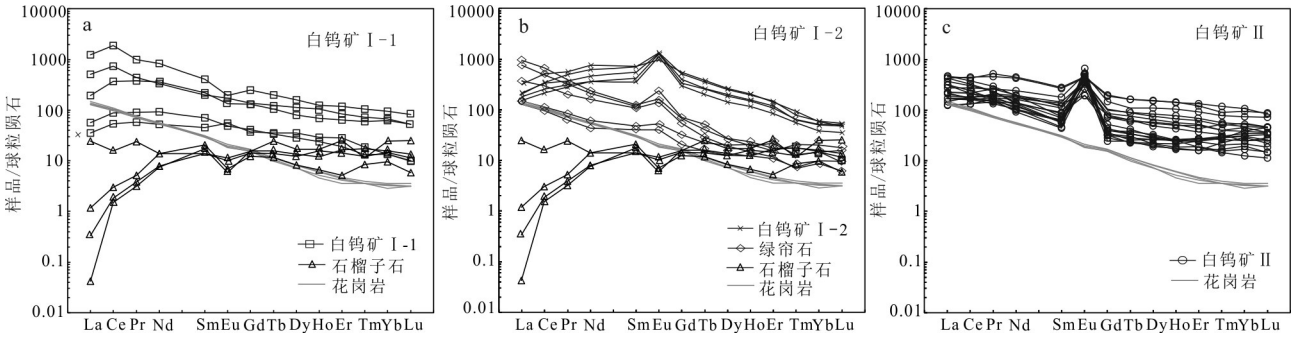

图5　永平Cu-W矿床3种类型白钨矿、石榴子石和绿帘石球粒陨石标准化稀土元素配分模式图(球粒陨石值来自 Sun et al., 1989; 花岗岩稀土元素数据来自 Zhang et al., 2018)

a. 白钨矿Ⅰ-1稀土元素配分模式;b. 白钨矿Ⅰ-2稀土元素配分模式;c. 白钨矿Ⅱ稀土元素配分模式

Fig.5　Chondrite-normalized REE patterns of garnet, epidote and different types of scheelite from the Yongping Cu-W deposit (The chondrite values are from Sun et al.,1989; The granite data are collected from Zhang et al., 2018)

a. REE patterns for Sch Ⅰ-1; b. REE patterns for Sch Ⅰ-2; c. REE patterns for Sch Ⅱ

1990; Rempel et al., 2009; Song et al., 2014; Xie et al., 2019)。在氧化条件下,Mo元素呈 Mo^{6+},以置换 W^{6+} 的方式进入白钨矿中;在还原条件下,Mo^{6+} 还原成 Mo^{4+},并以辉钼矿形式沉淀。永平Cu-W矿床中矽卡岩阶段到硫化物阶段,白钨矿中Mo含量逐渐降低(图6a),也反映了成矿过程氧逸度的降低。这一特征与安徽东顾山、西藏努日、安徽逍遥-百丈崖等典型矽卡岩钨矿或含钨多金属矿床相似(Song et al., 2014;聂利青等,2017)。

Eu作为变价元素,可以 Eu^{3+} 或者 Eu^{2+} 置换白钨矿中的 Ca^{2+}。当Eu以 Eu^{3+} 形式出现时,它的行为像其他三价稀土元素一样,并且与 Eu_N* 呈正相关,出现负Eu异常。在这种情况下,白钨矿中观察到的任何Eu异常都是继承于成矿流体中Eu的特征;当Eu以 Eu^{2+} 形式出现时,Eu^{2+} 更倾向于置换 Ca^{2+} 进入到白钨矿中,且替换行为与三价Sm和Gd元素不一致,所以Eu与 Eu_N* 无相关性,白钨矿球粒陨石标准化稀土元素配分图种呈现正Eu异常(Ghaderi et al., 1999)。因此,Eu异常能够指示成矿流体的氧化还原性(Ghaderi et al., 1999; Brugger et al., 2000; Song et al., 2014)。如图6b,白钨矿Ⅰ-1大致沿着虚线分布,表明Eu主要以 Eu^{3+} 形式出现,成矿流体为氧化性。如图6b,白钨矿Ⅰ-2和白钨矿Ⅱ显示与 Eu_N* 无相关性,说明Eu主要以 Eu^{2+} 形式出现,成矿流体为还原性。白钨矿中Mo含量及对应的Eu异常表明永平矿床从矽卡岩阶段到石英-硫化物阶段,成矿流体氧逸度逐渐减弱。

4.2　白钨矿地球化学对矿床成因指示

关于永平Cu-W矿床成因的争议是它是海底喷流沉积+热液改造型矿床还是矽卡岩型矿床。争议的焦点主要集中在成矿时代(石炭系还是晚侏罗世)和成矿物质来源(沉积地层还是岩浆岩)2个方面(徐克勤等,1996;赵常胜,2001;Gu et al., 2007;毛景文等,2009;Ni et al., 2017)。

前人研究表明,不同矿床类型的白钨矿具有不同的地球化学性质,可以利用白钨矿的微量元素和稀土元素特征来判断矿床类型(Ghaderi et al., 1999; Song et al., 2014; Poulin et al., 2018)。永平Cu-W矿床白钨矿呈明显的轻稀土元素富集模式(LREE/HREE比值为3.01~24.29),与典型矽卡岩型白钨矿右倾配分模式相一致,如赣东北朱溪(LREE/HREE比值为2~84;Yuan et al., 2019)、安徽东顾山(LREE/HREE比值为3~30;聂利青等,2017)等典型矽卡岩型钨矿床,而明显不同于石英脉型矿床中白钨矿的中稀土元素或重稀土元素富集模式(LREE/HREE比值为0.20~3.00, Ghaderi et al., 1999; Brugger et al., 2000)。并且永平白钨矿呈轻稀土元素富集、重稀土元素亏损的右倾模式(LREE/HREE比值为3.01~24.29),与似斑状黑云母花岗岩的稀土元素配分模式一致(LREE/HREE比值为17.16~20.23, Zhang et al., 2018)(图5a~c),表明其与花岗岩有关系。石榴子石稀土元素含量较低(20.8×10^{-6}~45.3×10^{-6}),并且绿帘石呈右倾稀土元素配分模式(LREE/HREE比值为7.33~27.15),表现出与白钨矿相似的稀土元

素配分模式(图 5b),因此这些矿物的沉淀对白钨矿的右倾配分模式影响不大。这些特征表明成矿流体保留了原始来源信息,并来源于花岗质岩浆。Song 等(2014)通过对中国东部鸡头山和百丈崖矽卡岩型W-Mo矿床的研究,得出石英脉型白钨矿 w(Mo)($<10\times10^{-6}$)远低于矽卡岩型白钨矿 w(Mo)($>7000\times10^{-6}$)。变质矿床通常形成于还原性环境,白钨矿中 Mo 含量低(Poulin et al., 2018)。相反,与岩浆有关的矿床更加氧化,白钨矿相对富集 Mo 元素,全球的 Mo 资源量主要来自于矿化的长英质岩体(Seedorff et al., 2005)。永平 Cu-W 矿床中白钨矿的 w(Mo)高(平均值为 10571×10^{-6}),且与赣东北朱溪、大湖塘、安徽逍遥-百丈崖等典型矽卡岩钨矿或含钨多金属矿床相似(图 6a,Song et al., 2014;Sun et al., 2017;Yuan et al., 2019)。此外,十字头岩体中 w(Mo)为 38.6×10^{-6},是地壳平均含量的 35 倍;叶家湾组地层中 w(Mo)为 0.78×10^{-6},是地壳平均含量的 0.7 倍(刘伯乐等,2016),笔者推断永平 Cu-W 矿床成矿流体来

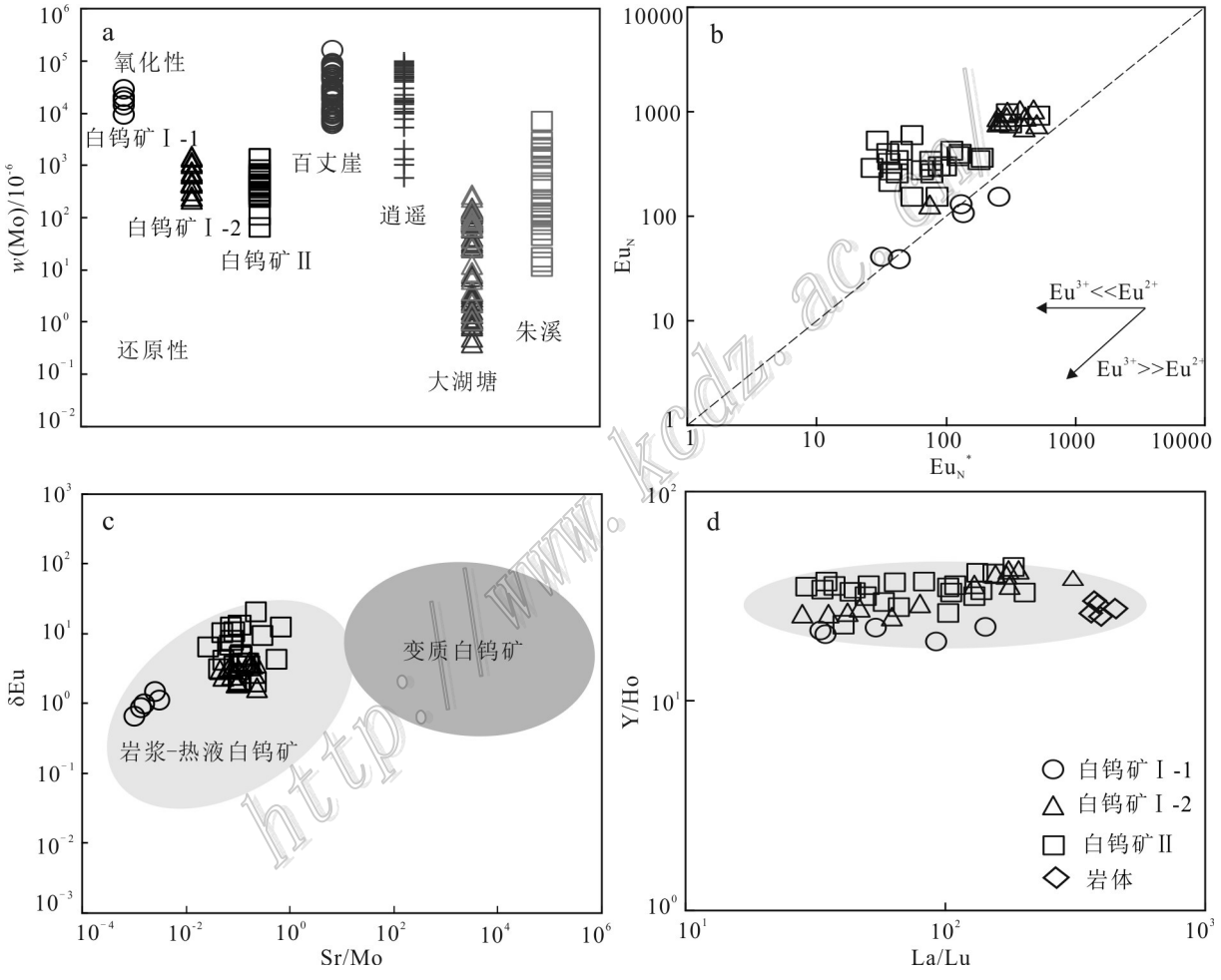

图6 永平 Cu-W 矿床白钨矿化学元素变化图

a. 永平白钨矿 w(Mo)与典型矽卡岩型矿床白钨矿 w(Mo)对比,数据来源于鸡头山和百丈崖矿床(Song et al., 2014),逍遥矿床(Su et al., 2020),朱溪矿床(Yuan et al., 2019),大湖塘矿床(Sun et al., 2017);b. 白钨矿 Eu_N*与 Eu_N关系图;c. Sr/Mo 与 δEu 关系图,底图据 Poulin et al., 2018;d. 白钨矿 La/Lu 与 Y/Ho 关系图

Fig. 6 Chemical variation of scheelite from the Yongping Cu-W deposit

a. Comparison of w(Mo) in different types of scheelite from the Yongping deposit with the scheelite data from the tungsten skarn deposits, including the Jitoushan and Baizhangya (after Song et al., 2014) and Xiaoyao (Su et al., 2020), the Zhuxi (after Yuan et al., 2019), the Dahutang (after Sun et al., 2017); b. Plot of Eu_N* versus Eu_N; c. Plot of Sr/Mo versus δEu. The base diagram after Poulin et al., 2018; d. Plot of La/Lu versus Y/Ho

源于十字头岩体。白钨矿稀土元素特征和Mo含量指示永平Cu-W矿床为矽卡岩型矿床。

Sr/Mo比值是常用来指示白钨矿形成环境的地球化学指标(Poulin et al., 2018; Sciuba et al., 2019)。在变质环境中,由于变质沉积岩可以释放出大量的Sr元素,因此变质环境中白钨矿含有较高的Sr/Mo比值(Sciuba et al., 2019),如新西兰Barewood矿床(Pitcairn et al., 2006)和云南大坪金矿床(熊德信等,2006)。相反,岩浆环境中,白钨矿来源于高度分异的长英质岩浆演化的含W流体,由于长英质岩浆亏损Sr元素,所以岩浆-热液矿床中白钨矿含有低的Sr/Mo比值(Poulin et al., 2018),如加拿大Cantung矿床(Laznicka, 2006)和中国东部朱溪矿床(Sun et al., 2019)。永平Cu-W矿床所有白钨矿Sr/Mo比值均落入岩浆-热液白钨矿区域,而明显区别于变质来源白钨矿的Sr/Mo比值范围(图6c),指示白钨矿可能来源于岩浆。由于相似的电荷和离子半径,Y与Ho具有相似的地球化学行为,并且在单一热液系统中相对稳定,可以用来指示成矿流体来源(Bau et al., 1992; Irber, 1999; Liu et al., 2019)。在本次研究中,矽卡岩型矿石中白钨矿Ⅰ和块状矿石中白钨矿Ⅱ的Y/Ho比值范围为19~43,并且均与似斑状黑云母花岗岩(Y/Ho=25~30)一致(图6d),明显不同于石炭系叶家湾组地层(Y/Ho=34~75;李二恒等,2012),说明成矿流体主要来源于岩浆,而不是石炭系灰岩。

永平矿区发育大量矽卡岩矿物并且具有分带性,从岩体到围岩,由石榴子石矽卡岩逐渐变为透辉石矽卡岩(田明君等,2014),这与典型矽卡岩型Cu矿床矽卡岩分带特征一致(Meinert et al., 2005)。结合前人研究成果,永平Cu-W矿床辉钼矿Re-Os年龄为156 Ma(李晓峰等,2007),与似斑状黑云母花岗岩锆石SIMS U-Pb年龄(160 Ma,丁昕等,2005)一致,表明永平成矿年龄在晚侏罗世,而不是石炭系。永平Cu-W矿床硫化物的硫同位素$\delta^{34}S$值介于−0.2‰~+1.9‰,明显不同于叶家湾组地层的$\delta^{34}S$值(−19.4‰~+8.4‰)(陈军军等,2016),与岩浆有关硫($\delta^{34}S$值=0±3‰;Chaussidon et al., 1990)接近,暗示具有岩浆硫来源的特征。如果一个岩浆-热液体系经历了W的富集,那么金红石中Ti可能被W置换,导致金红石在结晶过程中记录了W的富集(宋世伟等,2018)。永平矿区似斑状黑云母花岗岩中金红石微量元素数据支持这一假设,金红石中w(W)平均为8393×10^{-6}(未发表数据),明显支持W的富集来源于岩浆-热液体系。白钨矿地球化学特征为永平Cu-W矿床的成因提供了新的制约。因此永平Cu-W矿床是一个晚侏罗世形成的矽卡岩型Cu-W矿床,而不是石炭纪形成的海底喷流沉积型矿床。

不同空间位置形成的同一种类型白钨矿稀土元素和微量元素也有一定变化规律。随着钻孔深度增加(钻孔ZK205),白钨矿Ⅰ-2与石榴子石、辉石、绿帘石共生组合(ZK-12,112 m),变为与石榴子石、绿泥石共生组合(ZK-14和ZK-15,141~146 m),轻稀土元素相对重稀土元素更加富集(LREE/HREE平均值分别为3.5和15.5),可能由于样品ZK-12中富集轻稀土元素的绿帘石沉淀导致(LREE/HREE平均值为16.6)。并且随着钻孔深度增加,矽卡岩矿石中白钨矿Ⅰ-2中Mo含量逐渐增加(w(Mo)平均值分别为717×10^{-6}和923×10^{-6})。

5　结　论

(1) 永平Cu-W矿床退化蚀变阶段发育暗色均质白钨矿Ⅰ-1和亮色均质白钨矿Ⅰ-2,石英-硫化物阶段发育的白钨矿Ⅱ具有环带结构。

(2) 白钨矿中Mo含量和Eu异常能够指示成矿流体氧化还原性。白钨矿Ⅰ-1富集Mo元素,并呈负Eu异常,指示氧化性;白钨矿Ⅰ-2和白钨矿Ⅱ中Mo含量减少,并且呈正Eu异常,指示成矿流体氧逸度降低。

(3) 白钨矿具有高Mo、低Sr特征,与岩浆热液白钨矿特征一致,而明显不同于变质来源的白钨矿,指示成矿流体来源于岩浆。

(4) 白钨矿的轻稀土元素富集模式和Y/Ho比值与似斑状黑云母花岗岩相似,指示成矿流体主要来源于岩浆。白钨矿的地球化学特征指示永平Cu-W矿床为矽卡岩型矿床。

致　谢　野外工作得到了江西省铜业集团永平分公司工作人员的帮助和支持;LA-ICP-MS白钨矿微量元素分析实验得到了国家测试中心李超老师的大力支持;在文章审稿过程中,审稿专家给予宝贵建议;在此一一表示感谢!

References

Bau M and Moeller P. 1992. Rare earth element fractionation in meta-

morphogenic hydrothermal calcite, magnesite and siderite[J]. Mineralogy and Petrology, 45 (3): 231-246

Brugger J, Bettiol A, Costa S, Lahaye Y, Bateman R, Lambert D and Jamieson D. 2000. Mapping REE distribution in scheelite using luminescence[J]. Mineralogical Magazine, 64(5): 891-903.

Cai Y T, Ni P, Wang G G, Pan J Y, Zhu X T, Chen H and Ding J Y. 2016. Fluid inclusion and H-O-S-Pb isotopic evidence for the Dongxiang Manto-type copper deposit, South China[J]. Journal of Geochemical Exploration, 171: 71-82.

Chaussidon M and Lorand J P. 1990. Sulphur isotope composition of orogenic spinel lherzolite massifs from Ariege (North-Eastern Pyrenees, France): An ion microprobe study[J]. Geochimica et Cosmochimica Acta, 54(10): 2835-2846.

Chen J F and Jahn B M. 1998. Crustal evolution of southeastern China: Nd and Sr isotopic evidence[J]. Tectonophysics, 284(1-2): 101-133.

Chen J J, Cao D H, Yang X L, Qiu C R, Wang X J and Kan Y S. 2016. Fluid inclusions and sulfur isotope of the Yongping copper-polymetallic deposit in Jiangxi Province[J]. Acta Geoscientica Sinica, 37(2): 163-173(in Chinese with English abstract).

Cottrant J F. 1981. Cristallochimie et géochimie des terres rares dans la scheelite: Application à quelques gisements francais[D]. Ph. D. thesis. France: University of Paris-Ⅵ.

Ding X, Jiang S Y, Ni P, Gu L X and Jiang Y H. 2005. Zircon SIMS U-Pb geochronology of host granitoids in Wushan and Yongping copper deposits, Jiangxi Province[J]. Geological Journal of China Universities, 11(3) : 383-389(in Chinese with English abstract).

Dostal J, Kontak D J and Chatterjee A. 2009. Trace element geochemistry of scheelite and rutile from metaturbidite-hosted quartz vein gold deposits, Meguma Terrane, Nova Scotia, Canada, Genetic implications[J]. Mineralogy and Petrology, 97(1-2): 95-109.

Ghaderi M, Palin J M, Campbell I H and Sylvester P J. 1999. Rare earth element systematics in scheelite from hydrothermal gold deposits in the Kalgoorlie-Norseman region, western Australia[J]. Econ. Geol., 94(3): 423-437.

Gu L X, Zaw K, Hu W H, Zhang K J, Ni P, He J X, Xu Y T, Lu J J and Lin C M. 2007. Distinctive features of Late Palaeozoic massive sulphide deposits in South China[J]. Ore Geology Reviews, 31(1-4): 107-138.

Hsu L C and Galli P E. 1973. Origin of the scheelite-powellite series of minerals[J]. Econ. Geol., 68(5): 681-696.

Irber W. 1999. The lanthanide tetrad effect and its correlation with K/Rb, Eu/Eu*, Sr/Eu, Y/Ho, and Zr/Hf of evolving peraluminous granite suites[J]. Geochimica et Cosmochimica Acta, 63 (3-4): 489-508.

Laznicka P. 2006. Giant metallic deposits: Future sources of industrial metals[M]. Berlin: Springer Verlag, 732.

Li E H, Liu J R, Ni P, Cai Y T, Zhao K D, Ye C L and Zhu X T. 2012. Geochemistry and sedimentary environment of the Late Carboniferous siliceous cherts from Yanshan County, Jiangxi Province[J]. Geological Journal of China Universities, 18(4): 735-744(in Chinese with English abstract).

Li X F, Watanabe Y and Qu W J. 2007. Textures and geochemical characteristics of granitic rocks in the Yongping climax-type Cu-Mo deposit, Jiangxi, southeastern China, and their alteration, mineralization and tectonic regime[J]. Acta Petrologica Sinica, 23(10): 2353-2365(in Chinese with English abstract).

Li Y, Selby D, Li X H and Ottley C J. 2018. Multisourced metals enriched by magmatic-hydrothermal fluids in stratabound deposits of the Middle-Lower Yangtze River metallogenic belt, China[J]. Geology, 46(5): 391-394.

Li Z X, Li X H, Zhou H and Kinny P D. 2002. Grenvillian continental collision in south China: New SHRIMP U-Pb zircon results and implications for the configuration of Rodinia[J]. Geology, 30(2): 163-166.

Linnen R L and Williams-Jones A E. 1990. Evolution of aqueous-carbonic fluids during contact metamorphism, wall-rock alteration, and molybdenite deposition at Trout Lake, British Columbia[J]. Econ. Geol., 85(5): 1840-1856.

Liu B, Li H, Wu Q H, Evans N J, Cao J Y, Jiang J B and Wu J H. 2019. Fluid evolution of Triassic and Jurassic W mineralization in the Xitian ore field, South China: Constraints from scheelite geochemistry and microthermometry[J]. Lithos, 330-331: 1-15.

Liu B L, Li Y and Liang J F. 2016. The direction and symbol of deep prospecting of the Yongping copper polymetallic deposit in the eastern part of Qinghang metallogenic belt[J]. Teclinology, 20(7): 164-165(in Chinese with English abstract).

Mao J W, Xie G Q, Guo C L, Yuan S D, Cheng Y B and Chen Y C. 2008. Spatial-temporal distribution of Mesozoic ore deposits in South China and their metallogenic settings[J]. Geological Journal of China Universities, 14(4): 510-526(in Chinese with English abstract).

Mao J W, Xie G Q, Cheng Y B and Chen Y C. 2009. Mineral deposit models of mesozoic ore deposits in South China[J]. Geological Review, 55(3): 347-354(in Chinese with English abstract).

Mao J W, Chen M H, Yuan S D and Guo C L. 2011. Geological characteristics of the Qinhang (or Shihang) metallogenic belt in South China and spatial-temporal distribution regularity of mineral deposits[J]. Acta Geologica Sinica, 85(5): 636-658(in Chinese with English abstract).

Mao J W, Pirajno F and Cook N. 2011a. Mesozoic metallogeny in East China and corresponding geodynamic settings—An introduction to the special issue[J]. Ore Geology Reviews, 43(1): 1-7.

Mao J W, Zhang J D, Pirajno F, Ishiyama D, Su H M, Guo C L and Chen Y C. 2011b. Porphyry Cu-Au-Mo-epithermal Ag-Pb-Zn-distal hydrothermal Au deposits in the Dexing area, Jiangxi Province, East China—A linked ore system[J]. Ore Geology Reviews, 43 (1): 203-216.

Mao J W, Cheng Y B, Chen M H and Pirajno F. 2013. Major types and time-space distribution of Mesozoic ore deposits in South China and their geodynamic settings[J]. Mineralium Deposita, 48: 267-294.

Mao J W, Pirajno F, Lehmann B, Luo M C and Berzina A. 2014. Distribution of porphyry deposits in the Eurasian continent and their corresponding tectonic settings[J]. Journal of Asian Earth Science, 79: 576-584.

Meinert L D, Dipple G and Nicolescu S. 2005. World skarn deposits[J]. Society of Economic Geologists, 100: 299-336.

Ni P, Tian J H, Zhu H F, Jiang S Y and Gu L X. 2005. Fluid inclusion studies on footwall stringer system mineralization of Yongping massive copper deposit, Jiangxi Province, China[J]. Acta Petrologica Sinica, 21(5): 1339-1346(in Chinese with English abstract).

Ni P, Wang G G, Cai Y T, Zhu X T, Yuan H X, Huang B, Ding J Y and Chen H. 2017. Genesis of the Late Jurassic Shizitou Mo deposit, South China: Evidences from fluid inclusion, H-O isotope and Re-Os geochronology[J]. Ore Geology Reviews, 81: 871-883.

Nie L Q, Zhou T F, Zhang Q M, Zhang M and Wang L H. 2017. Trace elements and Sr-Nd isotopes of scheelites: Implications for the skarn tungsten mineralization of the Donggushan deposit, Anhui Province, China[J]. Acta Petrologica Sinica, 33(11): 3518-3530(in Chinese with English abstract).

Pitcairn I K, Teagle D A, Craw D, Olivo G R, Kerrich R and Brewer T S. 2006. Sources of metals and fluids in orogenic gold deposits: Insights from the Otago and Alpine schists, New Zealand[J]. Econ. Geol., 101(8): 1525-1546.

Poulin R S, Kontak D J, McDonald A, Beth M and McCLenaghan B M. 2018. Assessing Scheelite as an ore-deposit discriminator using its trace-element REE chemistry[J]. The Canadian Mineralogist, 56(3): 265-302.

Rempel K U, Williams-Jones A E and Migdisov A A. 2009. The partitioning of molybdenum (Ⅵ) between aqueous liquid and vapour at temperatures up to 370°C[J]. Geochimica et Cosmochimica Acta, 73(11): 3381-3392.

Sciuba M, Beaudoin G, Grzela D and Makvandi S. 2019. Trace element composition of scheelite in orogenic gold deposits[J]. Mineralium Deposita, 55(6): 1-24.

Seedorff E, Dilles J H, Proffett J M, Einaudi M T, Zurcher L, Stavast W J A, Johnson D A and Barton M D. 2005. Porphyry deposits: Characteristics and origin of hypogene features[J]. Society of Economic Geologists, 100: 251-298.

Shu L S. 2012. An analysis of principal features of tectonic evolution in South China Block[J]. Geological Bulletin of China, 31(7): 1035-1053(in Chinese with English abstract).

Song G X, Qin K Z, Li G M, Evans N J and Chen L. 2014. Scheelite elemental and isotopic signatures: Implications for the genesis of skarn-type W-Mo deposits in the Chizhou Area, Anhui Province, Eastern China[J]. American Mineralogist, 99(2-3): 303-317.

Song S W, Mao J W, Xie G Q, Song H, Chen G H, Rao J F and Ouyang Y P. 2018. Identification of ore-related granitic intrusions in W skarn deposits: A case study of giant Zhuxi W skarn deposit[J]. Mineral Deposits, 37(5): 940-960(in Chinese with English abstract).

Su Q W, Mao J W, Sun J, Zhao L H and Xu S F. 2020. Geochemistry and origin of scheelites from the Xiaoyao tungsten skarn deposit in the Jiangnan tungsten belt, SE China[J]. Minerals. 10(3): 1-22.

Sun K K and Chen B. 2017. Trace elements and Sr-Nd isotopes of scheelite: Implications for the W-Cu-Mo polymetallic mineralization of the Shimensi deposit, South China[J]. American Mineralogist, 102(5): 1114-1128.

Sun K K, Chen B and Deng J. 2019. Ore genesis of the Zhuxi supergiant W-Cu skarn polymetallic deposit, South China: Evidence from scheelite geochemistry[J]. Ore Geology Reviews, 107: 14-29.

Sun S S and McDonough W F. 1989. Chemical and isotopic systematics of oceanic basalts: implications for mantle composition and processes[M]. Geological Society of London, Special Publication. 313-345.

Sun W D, Zhang H, Ling M X, Ding X, Chung S L, Zhou J and Fan W. 2011. The genetic association of adakites and Cu-Au ore deposits[J]. International Geology Review, 53(5-6): 691-703.

Tian M J, Li Y G, Wan H Z, Zhang Y and Gao T T. 2014. Characteristics of skarn minerals in Yongping copper deposit, Jiangxi Province, and geological significances[J]. Acta Petrologica Sinica, 30 (12): 3741-3758(in Chinese with English abstract).

Tian M J, Li Y G, Miao L C, Zhang Y, Gao T T, Guo J H, Xue J Z and He B. 2019. Alteration and mineralization zoning, ore textures and ore-forming process of Yongping copper deposit, Jiangxi Province[J]. Acta Petrologica Sinica, 35(6): 1924-1938(in Chinese with English abstract).

Tomschi H P, Oberthür T, Saager R and Kramers J. 1986. Geochemical and mineralogical data on the genesis of the Mazowe gold field in the Harare Bindura greenstone belt, Zimbabwe[C]. Geocongress' 86, Johannesburg, South Africa 1986, Extended Abstracts, 345-348.

Wang G G, Ni P, Wang R C, Zhao K D, Chen H, Ding J Y, Zhao C and Cai Y T. 2013. Geological, fluid inclusion and isotopic studies of the Yinshan Cu-Au-Pb-Zn-Ag deposit, South China: Implications for ore genesis and exploration[J]. Journal of Asian Earth Sciences, 74: 343-360.

Xie G Q, Mao J W and Zhao H J. 2011. Zircon U-Pb geochronological and Hf isotopic constraints on petrogenesis of Late Mesozoic intrusions in the southeast Hubei Province, Middle-Lower Yangtze river belt, East China[J]. Lithos, 125(1-2): 693-710.

Xie G Q, Mao J W, Leon B, Fu B and Zhang Z Y. 2019. Mineralogy and titanite geochronology of the Caojiaba W deposit, Xiangzhong metallogenic province, southern China: Implications for a distal reduced skarn W formation[J]. Mineralium Deposita, 54(3): 459-472.

Xiong D X, Sun X M, Shi G Y, Wang S W, Gao J F and Xue T. 2006. Trace elements, rare earth elements (REE) and Nd-Sr isotopic compositions in scheelites and their implications for the mineralization in Daping gold mine in Yunnan Province, China[J]. Acta Petrologica Sinica, 22(3): 733-741(in Chinese with English abstract).

Xu K Q, Wang H N, Zhou J P and Zhu J C. 1996. A discussion on the

exhalative sedimentary massive sulfide deposits of South China[J]. Geological Journal of China Universities, 2(3): 241-256(in Chinese with English abstract).

Yu Z S, Zheng W B and Zheng Z C. 2016. Supplementary exploration report of the copper ploymetallic ore deposit in the deep of Yongping district, Qianshan Country, Jiangxi Province[R]. Northeast Jiangxi Geological Team of Jiangxi Bureau of Geological and Mineral Exploration(in Chinese).

Yuan L L, Chi G X, Wang M Q, Li Z H, Xu D R, Deng T, Geng J Z, Hu Y and Zhang L. 2019. Characteristics of REEs and trace elements in scheelite from the Zhuxi W deposit, South China: Implications for the ore-forming conditions and processes[J]. Ore Geology Reviews, 109: 585-597.

Yuan S D, Mao J W, Zhao P L and Yuan Y B. 2018. Geochronology and petrogenesis of the Qibaoshan Cu-polymetallic deposit, northeastern Hunan Province: Implications for the metal source and metallogenic evolution of the intracontinental Qinhang Cu-polymetallic belt, South China[J]. Lithos, 302-303: 519-534.

Zhang Y, Shao Y J, Liu Q Q, Chen H Y, Quan W and Sun A X. 2018. Jurassic magmatism and metallogeny in the eastern Qin-Hang Metallogenic Belt, SE China: An example from the Yongping Cu deposit[J]. Journal of Geochemical Exploration, 186: 281-297.

Zhao C S. 2001. The feature of synggenetic plume-sedimentation in Yongping copper deposit, Jiangxi[J]. Copper Engineering, (3): 48-50(in Chinese with English abstract).

Zhu X T, Ni P, Wang G G, Cai Y T, Chen H and Pan J Y. 2016. Fluid inclusion, H-O isotope and Pb-Pb age constraints on the genesis of the Yongping copper deposit, South China[J]. Journal of Geochemical Exploration, 171: 55-70(in Chinese with English abstract).

附中文参考文献

陈军军, 曹殿华, 杨昔林, 邱昌容, 王训军, 阚迎松 . 2016. 江西永平铜多金属矿床流体包裹体及硫同位素研究[J]. 地球学报, 37(2): 163-173.

丁昕, 蒋少涌, 倪培, 顾连兴, 姜耀辉 . 2005. 江西武山和永平铜矿含矿花岗质岩体锆石 SIMS U-Pb 年代学[J]. 高校地质学报, 11(3): 383-389.

田明君, 李永刚, 苗来成, 张宇, 高婷婷, 郭敬辉, 薛俊召, 何斌 . 2019. 江西永平铜矿床蚀变矿化分带、矿石组构及成矿过程[J]. 岩石学报, 35(6): 1924-1938.

李二恒, 刘家润, 倪培, 蔡逸涛, 赵葵东, 叶春林, 朱筱婷 . 2012. 江西铅山晚石炭世硅质岩地球化学 特征与沉积环境[J]. 高校地质学报, 18(4): 735-744.

李晓峰, Watanabe Y, 屈文俊 . 2007. 江西永平铜矿花岗质岩石的岩石结构、地球化学特征及其成矿意义[J]. 岩石学报, 23(10): 2353-2365.

刘伯乐, 李阳, 梁剑锋 . 2016. 钦杭成矿带东段永平铜多金属矿区深部找矿方向及标志[J]. 大科技, 20(7): 164-165.

毛景文, 谢桂青, 郭春丽, 袁顺达, 程彦博, 陈毓川 . 2008. 华南地区中生代主要金属矿床时空分布规律和成矿环境[J]. 高校地质学报, 14(4): 510-526.

毛景文, 谢桂青, 程彦博, 陈毓川 . 2009. 华南地区中生代主要金属矿床模型[J]. 地质论评, 3: 347-354.

毛景文, 陈懋弘, 袁顺达, 郭春丽 . 2011. 华南地区钦杭成矿带地质特征和矿床时空分布规律[J]. 地质学报, 85(5): 636-658.

倪培, 田京辉, 朱筱婷, 凌洪飞, 蒋少涌, 顾连兴 . 2005. 江西永平铜矿下盘网脉状矿化的流体包裹体研究[J]. 岩石学报, 21(5): 1339-1346.

聂利青, 周涛发, 张千明, 张明, 汪龙虎 . 2017. 安徽东顾山钨矿床白钨矿主微量元素和 Sr-Nd 同位素特征及其对成矿作用的指示[J]. 岩石学报, 33(11): 3518-3530.

舒良树 . 2012. 华南构造演化的基本特征[J]. 地质通报, 31(7): 1035-1053.

宋世伟, 毛景文, 谢桂青, 宋昊, 陈国华, 饶建锋, 欧阳永棚 . 2018. 矽卡岩型钨矿床成矿相关岩体识别——以江西景德镇朱溪超大型矽卡岩型钨矿床为例[J]. 矿床地质, 37(5): 940-960.

田明君, 李永刚, 万浩章, 张宇, 高婷婷 . 2014. 江西永平铜矿矽卡岩矿物特征及其地质意义[J]. 岩石学报, 30(12): 3741-3758.

田明君, 李永刚, 苗来成, 张宇, 高婷婷, 郭敬辉, 薛俊召, 何斌 . 2019. 江西永平铜矿床蚀变矿化分带、矿石组构及成矿过程[J]. 岩石学报, 35(6): 1924-1938.

熊德信, 孙晓明, 石贵勇, 王生伟, 高剑锋, 薛婷 . 2006. 云南大坪金矿白钨矿微量元素、稀土元素和 Sr-Nd 同位素组成特征及其意义[J]. 岩石学报, 22(3): 733-741.

徐克勤, 王鹤年, 周建平, 朱金初 . 1996. 论华南喷流-沉积块状 硫化物矿床[J]. 高校地质学报, 2(3): 241-256.

余祖寿,郑文斌, 郑忠超 . 2016. 江西省铅山县永平铜矿深部扩界区铜多金属矿补充勘探报告[R]. 江西省地质矿产勘查开发局赣东北大队 .

赵常胜 . 2001. 江西永平铜矿床以喷流成矿为主体的成因特征[J]. 铜业工程, (3): 48-50.